



Article

# Physical Processes Occurring in Dispersed Media with Carbon Nanomaterials under the Influence of Ultrasonification

Svetlana Obukhova <sup>1,\*</sup>  and Evgenii Korolev <sup>2</sup>

<sup>1</sup> Department of Urban Planning, Institute of Architecture and Urban Planning, Moscow State University of Civil Engineering, 129337 Moscow, Russia

<sup>2</sup> St. Petersburg State University of Architecture and Civil Engineering, 190005 St. Petersburg, Russia

\* Correspondence: shehovtsovasyu@mgsu.ru

**Abstract:** The up-to-date carbon nanoparticle application in materials science and composites is mostly represented by controlling of different methods of structure formation including incorporation of nanomaterials or nano-modifiers. The efficiency of such methods depends on disagglomeration and the distribution degree of the carbon nanoparticle within a dispersion medium, which are critical parameters to produce a composite with improved performance. At the same time, common approaches such as a surface activation or using surfactants do not guarantee a homogeneous dispersion of carbon nanoparticles. This research reports on a theoretical analysis of physical processes which take place during the ultrasonic treatment which is a widely used method for dispersion of nanomaterials. The experimental data demonstrate an efficiency of the proposed method and prove the theoretical assumptions. The theoretical analysis performed in this study can be applied to implement and scale-up the process using sonicators. It was established that ultrasonic treatment has a more intensive effect in an organic hydrocarbon medium. So, in industrial oil, the heating rate from ultrasonification is 20 °C/min, in residual selective purification extract, it is 33 °C/min. For aqueous systems, the heating rate from ultrasonification is significantly lower and amounts to 2 °C/min for suspensions with Sulfanol and 11 °C/min for suspensions with ViscoCrete 2100. It was established that in the studied dispersed systems (aqueous solutions with surfactants and organic medium), there is no directly proportional dependence of the amount of heating of suspensions on the duration of ultrasound dispersion (USD), which is caused by ultrasonic dispersion not under adiabatic conditions, as well as the dependence of absorption coefficient of ultrasonic energy for dispersed systems on parameters of system structure.

**Keywords:** polymer-modified binder; cement composite; carbon nanotubes ultrasonification; surface tension; temperature



**Citation:** Obukhova, S.; Korolev, E. Physical Processes Occurring in Dispersed Media with Carbon Nanomaterials under the Influence of Ultrasonification. *C* **2023**, *9*, 18. <https://doi.org/10.3390/c9010018>

Academic Editor: Jandro L. Abot

Received: 23 December 2022

Revised: 12 January 2023

Accepted: 19 January 2023

Published: 31 January 2023



**Copyright:** © 2023 by the authors. Licensee MDPI, Basel, Switzerland. This article is an open access article distributed under the terms and conditions of the Creative Commons Attribution (CC BY) license (<https://creativecommons.org/licenses/by/4.0/>).

## 1. Introduction

The use of carbon nanomaterials significantly affects the properties of building materials, especially in concrete and asphalt concrete. The merits of using carbon nanomaterials are to achieve extraordinary quality indicators. For example, the introduction of carbon nanotubes into concrete makes it possible to effectively fill pores in concrete [1]. This provides a significant increase in the strength of concrete. It also ensures the impermeability of salts and improves durability [1]. However, if carbon nanotubes are poorly dispersed, they tend to agglomerate [2]. This leads to the absorption of more water in the cement composite. Then the water evaporates, leaving pores that reduce the strength [3]. The properties of asphalt concrete directly depend on the properties of bitumen. So, a lot of research is directed to the modification of bitumen. This makes it possible to improve the properties of asphalt concrete. The introduction of carbon nanotubes into a bitumen binder improves the structure of the system, increases high-temperature properties and resistance to thermooxidative aging [4]. In addition, researchers have noted an improvement in

low-temperature and high-temperature rheological properties [5]. However, at present, achieving a homogeneous dispersion with nanoscale particles is a problem that inhibits the development of nanomodification [6]. The analysis of the physical processes of dispersed systems with carbon nanomaterials is very difficult. This is due to the appearance of dimensional effects arising from the anomaly of the characteristics of nanoparticles, as well as the peculiarity of the interaction between them [7,8]. The presence of the dependence of some properties of matter on the size of the object from which it consists of (the size effect [9]) makes it possible to actively affect the processes of structure formation in the field of materials science and to obtain materials with properties substantially exceeding the properties of analogues. The current stage of development of nanotechnology in materials science is based on the regulation of the processes of structure formation through the introduction of primary nanomaterials [10] that are naturally prone to aggregation. The effect of their introduction for bulk materials should depend both on the size of the agglomerate of primary nanomaterials and on the uniformity of their distribution in the component that forms the performance properties of the composite (in a matrix that can be formed from a mixture of binder and activator or substance that acquires strength after thermal exposure or when changing external physical conditions). The mechanisms of the participation of primary nanoscale materials in the structure formation of composites depend on the nature of the modified matrix (binder) and is under study. For mineral binding systems, it is assumed that the main mechanism consists during heterogeneous nucleation, the conditions of which appear to be determined by nucleation on active nuclei:

$$\frac{W_{get}}{W_{gom}} = 1 - \left( \frac{\sigma_f}{\sigma_h} \right) \cos \theta, \quad (1)$$

where  $W_{get}$ —heterogeneous nucleation work;  $W_{gom}$ —homogeneous nucleation work;  $\sigma_f$  and  $\sigma_h$ —the surface tension of the wetting liquid phase and the solid surface, respectively;  $\theta$ —the wetting angle. This solution differs significantly from the classical solution proposed by Volmer M. (1939).

$$\frac{W_{get}}{W_{gom}} = \frac{1}{2} - \frac{3}{4} \cos \theta + \frac{1}{4} \cos^3 \theta, \quad (2)$$

which shows that the work of heterogeneous nucleation is always less than the work of homogeneous nucleation at  $\theta < 180^\circ$ . For heterogeneous nucleation on active nuclei (this representation is the most accurate representation of the influence of particles of primary nanomaterials), the range of variation in the ratio  $W_{get}/W_{gom}$  is significantly smaller and the predominance of heterogeneous nucleation over homogeneous is manifested at  $\theta < 90^\circ$ .

Ultrasound is most often used to disperse solid particle and distribute carbon nanomaterials in the volume of the carrier medium. The interaction of ultrasound with the medium is a relatively well-studied process. However, the effects that arise in apparatuses in the reflection and refraction of waves, as well as when heating the medium, determine the individual features for each apparatus of ultrasonic treatment. The mentioned effects and cavitation phenomena help to reduce the frequency of ultrasound required for dispersion. The approximate calculations without cavitation indicate that the ultrasound frequency for dispersion to objects smaller than 100  $\mu\text{m}$  must be more than 40 GHz (at a propagation speed of 2000 m/s). It is generally known that dispersion naturally increases the interfacial surface of the reactants. The external surface of the initial aggregate is [10]:

$$S'_{arp} = \pi \eta_f (D_o - d_o)^2, \quad (3)$$

where  $D_o$ —the size of the aggregate;  $d_o$ —the diameter of the nanoparticle;  $\eta_f$ —the particle packing density in the aggregate. On this surface, there are particles in the quantity of:

$$N'_o = S' / \bar{s}_o = 4 \eta_f \left( \frac{D_o}{d_o} - 1 \right)^2, \quad (4)$$

where  $\bar{s}_0 = \pi d_0^2/4$ —the projection of one particle onto the surface. After the destruction of the aggregate (the process of dispersion), the total surface of the particles will be equal to:

$$S = N\pi d_0^2, \quad (5)$$

where  $N$ —the number of particles included in the aggregate. In the work of Elpiner I.E. [11], one of the mechanisms of intensification of processes in liquid media was determined, composed of cavitation fluctuations in the liquid and accompanied by powerful microcurrents, sound pressure and a sound wind which “washes” the boundary layer. This eliminates the resistance to the transfer of reacting substances. Ultrasonic cavitation is a catalyst for the occurring of physical and chemical processes. Its implementation is possible due to the transformation of low ultrasonic energy density into high in the vicinity and inside the gas bubble, which causes it to close at a pressure of about hundreds of MPa [12]. This ensures strong hydrodynamic disturbances in the fluid due to the formation of a shock wave. The lens-like shape of the bubble desensitizes the appearance of a high-voltage microdot charge. This initiates intense radiation of acoustic waves; a complex hydrodynamic situation arises. All this is accompanied by the destruction of the surface of solids, which border on the cavitating liquid [13].

The formation of sonochemical processes was discovered more than 60 years ago. However, to date, the authentic nature of the primary act of the indicated process has not been established. The main factors influencing the sonochemical reactions rate [13,14] are the intensity of ultrasonic energy per unit area of the radiator in the sounded medium. The beginning of the reaction occurs at a certain threshold of intensity of ultrasonic oscillations which coincides with the beginning of cavitation. After the threshold of intensity is exceeded, the reaction rate decreases sharply. At low frequencies of ultrasonic vibrations, cavitation begins and proceeds at lower intensities. To ensure the destruction of the unit, it is necessary to spend energy. Including the  $E_k$ , energy required to overcome the adhesion forces between particles, the energy cost for wetting the formed surface  $E_s$ , to overcome the forces of medium resistance when moving particles  $E_c$ :

$$E = E_k + E_c + E_s, \quad (6)$$

The effect of ultrasonification is directed at moving particles over large distances from one another, and provided that  $d_0 \ll \lambda$  (wavelength), the force [15] acts on the particles:

$$F_p = 4\pi \left(\frac{d_0}{2}\right)^2 E \left(\frac{k_\lambda d_0}{2}\right)^4 \frac{1 + (1 - \delta)^2}{(2 + \delta)^2}, \quad (7)$$

where  $k_\lambda$ —the wavenumber;  $E$ —the time-average energy density of the acoustic field;  $\delta = \rho / \rho_f$ ;  $\rho$ —the density of the medium;  $\rho_f$ —the density of the modifier substance that causes the particle to oscillate with the wave. The forces of Bjerknes, acting on individual particles in an extended aggregate, will facilitate their mutual attraction:

$$F_B = 4\pi\rho \left(\frac{d_0}{2}\right)^4 \frac{v^2}{h^2} \cos \varphi, \quad (8)$$

where  $v$ —the vibrational speed;  $\varphi$ —the phase shift of particle pulsation;  $h$ —the particle separation. In a complex hydrodynamic situation, with intensive emission of acoustic waves Bernoulli forces arise, which also are directed to the attraction of particles in a medium:

$$F_B = 4\pi\rho \left(\frac{d_0}{2}\right)^4 \frac{v^2}{h^2} \cos \varphi, \quad (9)$$

where  $v$ —the particle velocity. In the process of ultrasonification, two groups of forces of different directions act. The first group is caused by cavitation processes, as its action

is aimed at destruction of units. The second group, caused by the forces of Bjerknes and Bernoulli, promotes their coagulation.

According to the results of the research of the group of authors [16], one of the main factors that have the greatest influence on the dispersing process is surface tension. Therefore, the nature of the interaction at the interface “medium-dispersed phase” is an additional factor that contributes to the effectiveness of ultrasonic dispersion. It is reasonable to assume that to ensure the production of homogeneous dispersions it is necessary to use lyophilic nanomaterials that are capable of intermolecular interaction with liquids that meet them. In this case, the Schukin–Rebinder criterion [17] is valid, according to which the spontaneous dispersion process is possible if the surface tension is a measure of the uncompensated molecular forces at the interphase boundary that meets the following condition.

$$\sigma_{12} \leq \gamma \frac{kT}{r^2}, \quad (10)$$

where  $\sigma_{12}$ —the surface tension at the interface between a liquid and a solid;  $\gamma$ —a constant ( $\gamma = 10 \dots 15$ );  $r$ —the radius of the particle;  $k$ —the Boltzmann constant;  $T$ —the temperature.

The thermodynamic equilibrium upon contact of a drop of liquid with a solid surface is determined by the minimum free surface energy of the system and is characterized by the value of the contact angle  $\theta$ . Thus, according to Young’s equation:

$$\frac{kT}{r^2} = \sigma_{23} - \sigma_{13} \cos \theta, \quad (11)$$

where  $\sigma_{23}$ —the surface tension at the “solid–gas” boundary;  $\sigma_{13}$ —the same as “liquid–gas”;  $\theta$ —the wetting contact angle. Considering the small value of  $\gamma \frac{kT}{r^2}$ , it is obvious that as  $\theta \rightarrow 180^\circ$  the condition:

$$\frac{\sigma_{23}}{\sigma_{13} \cos \theta} = 1, \quad (12)$$

is not met, and when  $\theta \rightarrow 0^\circ$  it is met only under condition:

$$\frac{\sigma_{23}}{\sigma_{13}} = 1, \quad (13)$$

This notation is only realized when a connection is formed at the phase boundary, whose properties are similar to those of the liquid phase. Summarizing the above presented material can be concluded. Spontaneous dispersion reinforced by Brownian motion is possible only if a solvate layer (shell) is formed at the interfacial boundary. Various combinations of nanoparticles and organic molecules make it possible to produce new materials with unique properties [18]. However, the effectiveness of the introduction of nanoparticles significantly depends not only on their type, dosage, but also on the technological parameters of modification [19]. Here, the most important aspect is to ensure the dispersion of CNTs and the stability of the resulting suspension [20].

For dispersion, the most promising method is ultrasonic dispersion, and there are a significant number of research papers studying this phenomenon [21–24]. The latest scientific results were summarized in the review article by Yadav et al. [25]. They showed that in this field of research there are “white spots” that make it difficult to scale nanotechnology industrially. Since carbon nanotubes have increased thermal conductivity, an increase in temperature occurs during ultrasonic dispersion. However, now there are no studies of the effect of temperature in the process of ultrasonic sounding on the medium containing carbon nanotubes, so this area requires additional research. Moreover, an important factor is the installation of a compatible environment. Thus, Manzetti et al. [26] reviewed and summarized information on dispersion methods in various media and reported that in organic solvents such as N-methyl pyrrolidone, DMF, 1,2-dichloroethane, ethanol, chloroform, acetone, diethyl ether, propanol, PVA, methanol, DMSO, 1-Naphthol, catechol (1,2-benzenediol), pyrogallol, tetracene, polyethers, THF, chlorosulfonic acid, and

crown ethers can be dispersed by CNT. However, there is no data on the stability of the obtained suspensions.

Due to the large specific surface area, porous structure and high adsorption capacity, carbon nanomaterials are widely used in gas purification [27–29], therefore, they have been extensively studied for gas systems and, to a much lesser extent, the features of interaction with liquids have been studied. Therefore, this study is aimed at eliminating gaps in the field of knowledge of the processes occurring in dispersed media under the influence of an ultrasonic wave in polar and nonpolar medium containing nanoparticles.

## 2. Materials and Methods

### 2.1. Raw Materials and Characterization

#### 2.1.1. Polar Medium

Multilayer fulleroid nanoparticles (MFN) (Figure 1), with a bulk density of  $0.6 \text{ g/cm}^3$ , and average size of 150 nm were obtained from STC Applied Nanotechnology (Moscow, Russia). To disperse MFN, an anionic surfactant, Sulfanol from LLC «Rushimtreid» (Moscow, Russia) was used. Table 1 summarizes the characteristics of the surfactant as provided by the manufacturer.

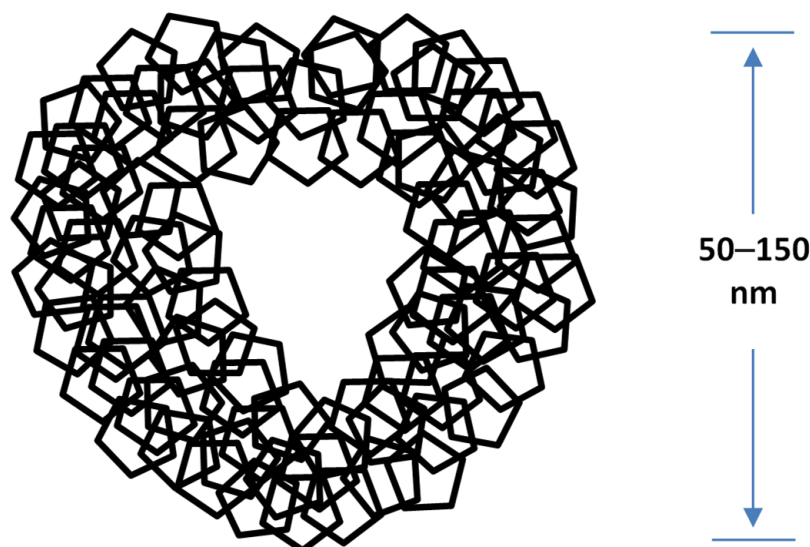


**Figure 1.** Schematic depiction of the structure of multilayer polyhedral nanoparticles.

**Table 1.** Surfactants' characteristics.

Property	Sulfanol	ViscoCrete 2100
pH (Sol. 10%)	7.5	4.5
Solubility (in water), %	total up to 95%	–
Humidity, %	5% max	–
Molecular weight, g/mol	348.48	–
Density, $\text{g/cm}^3$	0.48	1.08

Carbon primary materials called functionalized multi-walled carbon nanotubes CN-PLUS (–COOH)—2% by weight (Figure 2), with a purity of 98% by weight, the diameter of the nanotubes in the source material is 10–60 nm, 10–30 microns long were obtained from LLC «Carbon Nanotubes Plus» (CNPLUS), USA. To disperse MWCNTS, an anionic-type surfactant based on polycarboxylate esters ViscoCrete 2100, manufactured by Sika Canada Inc. (Pointe-Claire, QC, USA) was used. Table 1 summarizes the characteristics of the surfactant as provided by the manufacturer.

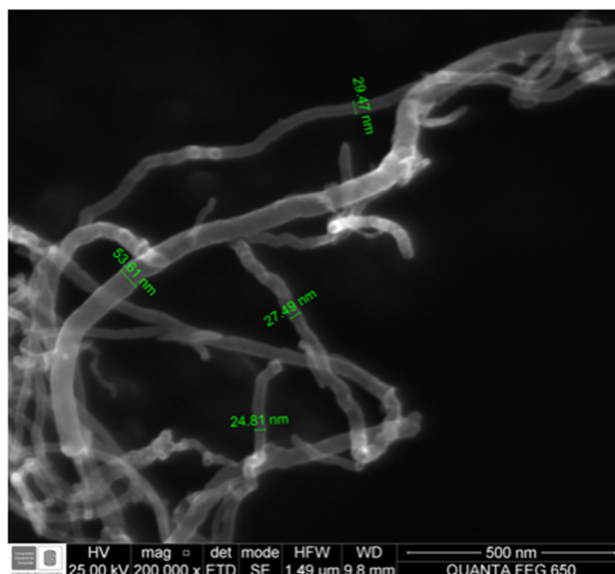


Figure 2. The structure of CNPLUS.

2.1.2. Non-Polar Medium

A standard organic solution of industrial oil, a mixture of hydrocarbons of paraffinic, naphthenic, and aromatic series was utilized as a carrying agent. Table 2 summarizes the group composition of the plasticizer as provided by the manufacturer. Multiwall carbon nanotubes (MWCNTS) in the form of filamentous formations of polycrystalline graphite with a bulk density of 0.5 g/cm<sup>3</sup> and an average size of 50 nm were produced and supplied by LLL «Nanotechcentr» (Tambov, Russia), Figure 3.

Table 2. Group composition of plasticizers.

Name of Components	Industrial Oil	Residual Selective Purification Extract
Paraffin—naphthenic hydrocarbons	68.30%	9.93%
Light aromatic hydrocarbons	7.50%	17.80%
Medium aromatic hydrocarbons	-	14.60%
Heavy aromatic hydrocarbons	19.20%	38.10%
Resins (total quantity)	5.00%	18.27%
Asphaltenes	-	1.30%

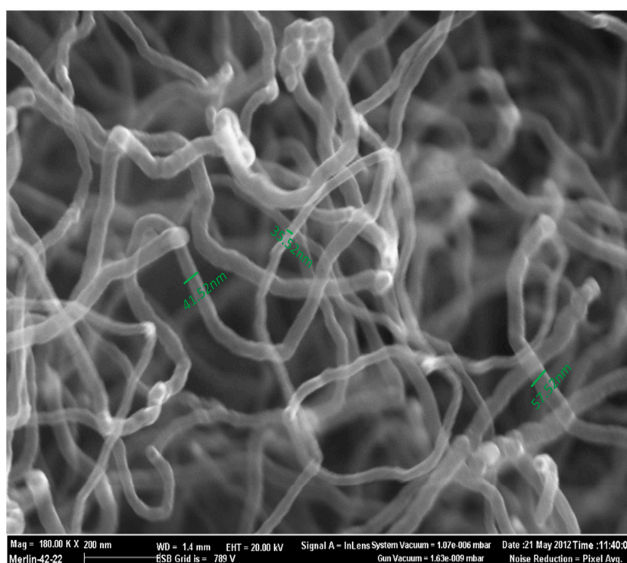
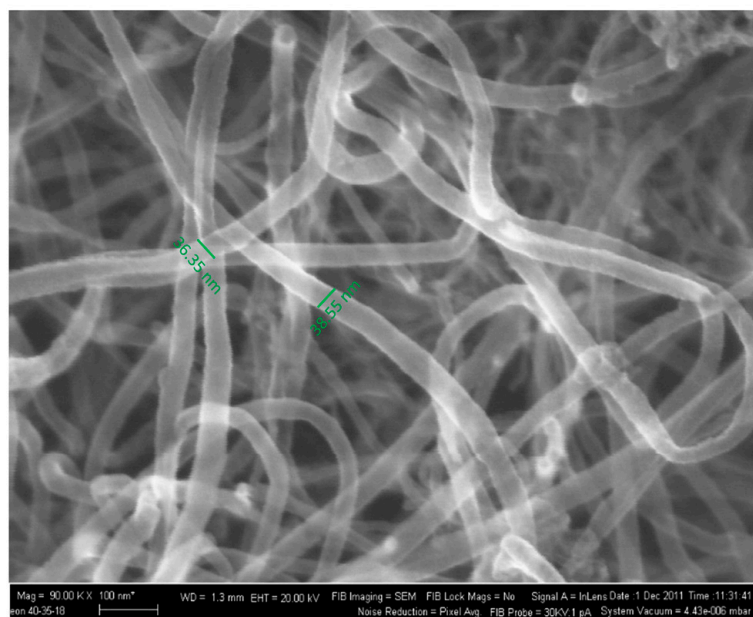


Figure 3. The structure of MWCNTS.

The product of oil refining called “residual selective purification extract” (RSPE) was produced by LLC «Lukoil International». The production technology is as follows: the tar from the vacuum part of the atmospheric-vacuum column goes to propane deasphaltize, where it is divided into asphalt and deasphaltize. Next, the deasphaltize enters the selective purification, where it is divided into a refined product, from which diesel fuel is obtained, and a residual selective purification extract. Table 2 summarizes the group composition of the plasticizer as provided by the manufacturer. Multiwall carbon nanotubes (MWCNT-MD) in the form of filamentous formations of polycrystalline graphite with a bulk density of  $0.06 \text{ g/cm}^3$  and an average size of 20 nm were produced and supplied by LLC «Nanotechcentr» (Tambov, Russia), Figure 4.



**Figure 4.** The structure of MWCNT-MD.

### 2.1.3. Building Materials

To test theoretical ideas about the effect of dispersion efficiency on the properties of the composite, a cement composite for polar media and a polymer-modified binder for nonpolar media were considered.

**Cement composite:** Argos cement, class 32.5 N (manufactured by Columbia) was used as a binder for the preparation of cement composite. Quartz river sand (Bucaramanga deposit, Colombia), grain size less than 5 mm, bulk density  $1529 \text{ kg/m}^3$ , water adsorption of sand 1.46%. Nano-modified aqueous solution of a surfactant.

**Polymer-modified binder:** bitumen 100/130, manufactured by LLC “Lukoil International”, with the following properties: the penetration depth of the needle is 0.1 mm, at a temperature of  $25 \text{ }^\circ\text{C}$  is  $112 \text{ mm}^{-1}$ ; the softening point is  $47 \text{ }^\circ\text{C}$ ; ductility at  $0 \text{ }^\circ\text{C}$  is 5.6 cm, the fragility temperature according to the Fraas method is  $-20 \text{ }^\circ\text{C}$ ; the change in the softening point of the sample after aging is 4% was used for the preparation of polymer-modified binder. Styrene-butadiene-styrene (SBS), divinyl styrene thermoplastic elastomer with a linear structure SBS 30L-01, corresponding to TU 38.40327-98, manufactured by LLC “Voronezhsintezkauchuk”, was used as a polymer. Nano-modified plasticizer.

### 2.2. Methods

Preparation of an aqueous dispersion (polar medium) of multilayer fulleroid nanoparticles with Sulfanol and aqueous dispersion of CNPLUS with ViscoCrete 2100 were achieved by premixing the composition with water at  $25 \text{ }^\circ\text{C}$  using an ultrasonic treatment for 1 min. Preparation of an organic dispersion of industrial oil (nonpolar medium) with MWCNTS and organic dispersion of residual selective purification extract with MWCNT-MD were

achieved by premixing with organic medium at 25 °C using a magnetic mixing blender for 1 min. Ultrasonic dispersion was performed with a Sonics Model Vibra-Cell 750. The surface tension of solutions ( $\sigma$ ) was determined with a Tensiometers KRUSS K100 using the Wilhelmy plate method, the testing temperature  $25 \pm 0.03$  °C. The dispersion degree was controlled using a laser analyzer Zetatrac NPA152—31A, which allows to reliably determine the particle sizes of up to 0.8  $\mu\text{m}$

### 2.2.1. Cement Composite

The selection of the ratio of components for the cement composite (cement: sand: aqueous surfactant solution) was carried out according to the ACI 211 method. The water-cement ratio was 0.5. The surfactant content correspond to the simultaneous achievement of the maximum reduction in the surface tension of the aqueous solution and the best workability of the mixture. The preparation of the mortar mixture was carried out in the following order. The laboratory mixer was used for mixing. Cement (450 g) was placed in the mixer bowl. Then various concentrations of carbon nanotubes were added to the mixing bowl with cement, which were previously dispersed in 225 mL of water. After that, the necessary amount of quartz river sand (1350 g) was added to the mixing bowl. The compressive strength of samples with dimensions of  $5 \times 5 \times 5$  cm prepared from cement mortar was determined by the INVE-323-07 method. The bending tensile strength of samples of beams with dimensions of  $4 \times 4 \times 16$  cm prepared from cement mortar was determined by the INV E-324-07 method. The results were obtained from the mean of 3 specimens for each test to decrease the possible errors.

### 2.2.2. Polymer Modified Binder

The control composition of a polymer-modified binder with a hydrocarbon plasticizer (without MWCNTs and MWCNT-MD) was selected by the authors earlier in the study [12]. The technology of preparation of polymer-modified binder consisted in the fact that the bitumen preheated to the operating temperature (150 °C) was blended with an organic medium in which MWCNTs or MWCNT-MD were previously dispersed. The producing melt was mixed with a paddle-type mixer at low speed for 5 min, then the polymer was added, and further mixing was carried out at a speed of 1000 rpm during 40–60 min until the polymer was completely dissolved in the volume. Then the producing polymer-modified binder was placed in a drying cabinet, at a temperature of 150 °C it was kept for 40–60 min to mature and structure the system.

The quality of polymer-modified binders was evaluated by physical, mechanical, and rheological quality indicators:

- the penetration depth of the needle,  $\text{mm}^{-1}$ , at a temperature of 0 °C and 25 °C (according to the Russian State Standard 11501 method);
- softening point by “Ring and ball”, °C (according to the Russian State Standard 11506 method);
- fragility temperature by Fraas method, °C (according to the Russian State Standard 11507 method);
- ductility, cm, at a temperature of 0 °C and 25 °C (according to the Russian State Standard 11505 method);
- change in the softening point after thermo-oxidative aging, °C (according to the Russian State Standard 18180 method);
- change in fragility temperature after thermo-oxidative aging, °C;
- dynamic viscosity, at a temperature of 135 °C (according to the Russian State Standard 33137 method), at a shear rate of  $90 \text{ s}^{-1}$ , on the Anton Paar Modular Compact Rheometer Physica MCR 101 device.

The flow chart of the research approach of this study is shown in Figure 5.

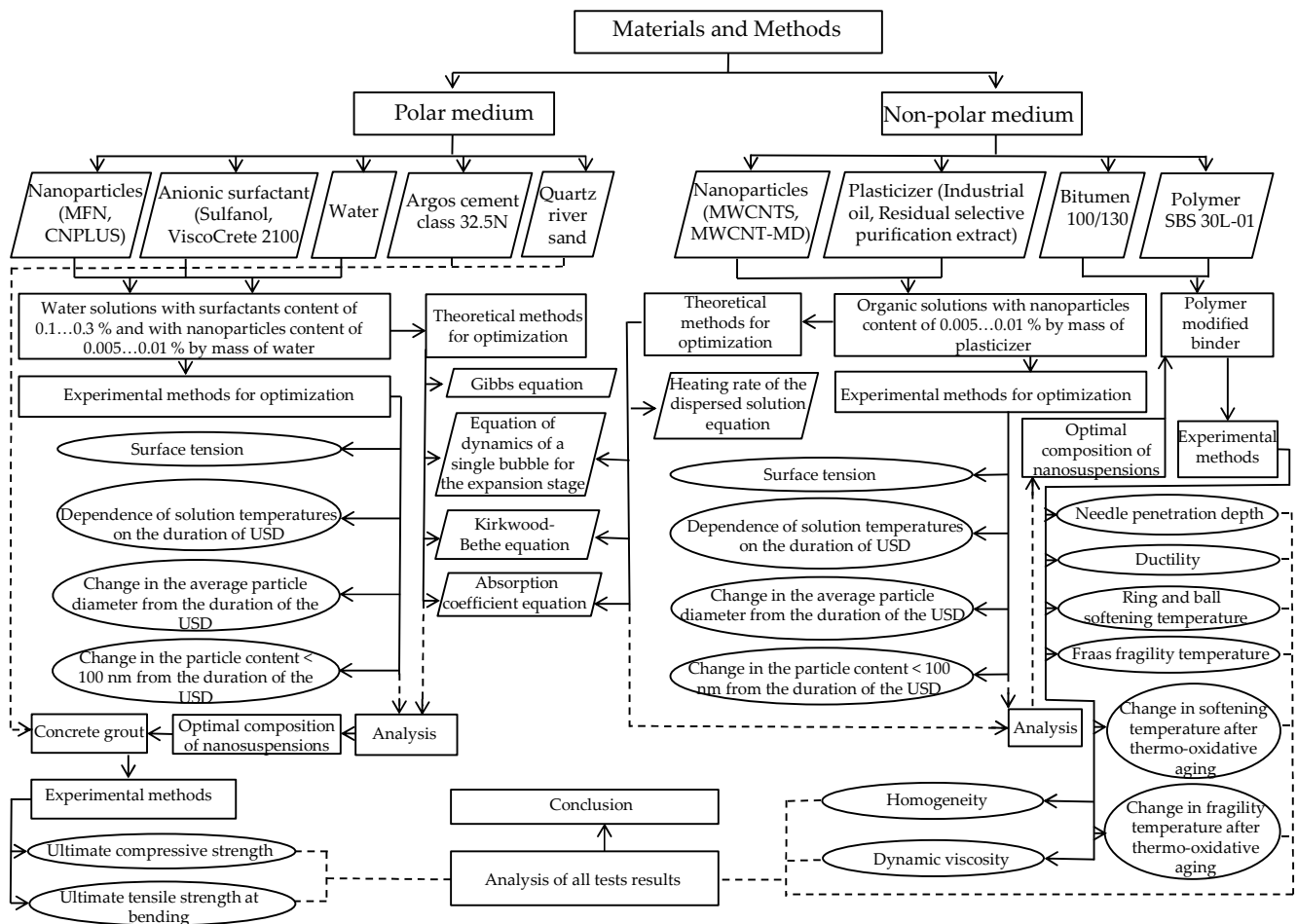


Figure 5. The flow chart of the research approach.

### 3. Results

Determination of the influence of ultrasonic treatment on the dispersed composition of nanomaterials was carried out on two different systems: (1) an aqueous solution comprising MFN [30] and Sulfanol [31] which is an anionic surfactant that adsorbs quite intensively on MFN, (Table 3) and a solution including CNPLUS carbon nanotubes with an anionic surfactants based on polycarboxylate esters of ViscoCrete 2100, (Table 4); (2) an organic solution comprising industrial oil with MWCNTS [32] and an organic solution comprising residual selective purification extract with MWCNT-MD, (Table 5).

Table 3. Dependence of surface tension on the concentration of Sulfanol and MFN.

Dosage of Sulfanol, %	Surface Tension, mN/m		
	$\sigma_0$ , mN/m	Dosage of MFN, %	
		0.005	0.01
0.0	72.75	72.75	72.75
0.1	58.26	63.35	65.02
0.2	45.95	52.71	54.11
0.3	36.75	47.61	49.53

It is known from mechanics that the equilibrium state of the system corresponds to the minimum value of its potential energy. For the system under consideration, this principle can be represented as follows: the energy of the surface tension forces tend towards zero. Analysis of the data (Tables 1–3) obtained confirmed the high adsorption activity of Sulfanol, and it was also found that the organic solution is characterized by a lower surface tension of 31.59 and 31.20 mN/m, respectively. When introducing MFN

(0.005% and 0.01%) into an aqueous solution of Sulfanol, the surface tension increases to 35%. When introducing CNPLUS nanoparticles (0.005% and 0.01%) into an aqueous solution of ViscoCrete 2100, the surface tension increases to 30%. An increase in the surface tension of aqueous solutions with anionic surfactants when nanoparticles are introduced indicates that surfactant molecules are adsorbed on the surface of nanoparticles (MFN and CNPLUS). The dispersed phase in this case is surface-active, and the absorbed surfactant will contribute to dispersion. It is worth noting that the amount of CNT in the studied range does not contribute to the major change in surface tension.

**Table 4.** Dependence of surface tension on the concentration of ViscoCrete 2100 and CNPLUS.

Dosage of ViscoCrete 2100, %	Surface Tension, mN/m			
	$\sigma_0$ , mN/m	Dosage of CNPLUS, %		
		0.005	0.01	
0.0	72.75	72.75	72.75	72.75
0.1	58.26	58.87	59.27	59.27
0.2	45.24	51.6	52.21	52.21
0.3	44.48	52.74	53.93	53.93

**Table 5.** Dependence of surface tension on the concentration of MWCNT and MWCNT-MD.

Name of Organic Solution	Surface Tension, mN/m			
	$\sigma_0$ , mN/m	Dosage of MWCNT, %		
		0.0005	0.005	0.05
Industrial oil	31.59	30.91	30.91	30.93
Residual selective purification extract	31.20	31.10	29.60	28.30

When studying suspensions on organic solutions, it was found that the application of MWCNT (from 0.0005% to 0.05%) in the industrial oil slightly reduces surface tension. It was found that the application of MWCNT-MD (from 0.0005% to 0.05%) in the RSPE reduces surface tension of up to 10%. Obviously, unlike aqueous solutions of surfactants, the mechanism of participation of the organic medium in dispersion is different. The surface tension reduction in the disperse extract system probably occurs under the molecular separation of the polymolecular medium because of interaction with MWCNT-MD.

Ultrasound dispersion was performed on a Vibra-Cell lab unit, which provides an output power of ultrasound at 500 W. When sounding nanomaterials, in addition to the sound field, the thermal energy generated by the absorption of ultrasound also affects the dispersed system, Figure 6.

It is seen from the presented dependences that the heating proceeds more intensively in the organic solution. So, after 6 min from the beginning of the USD, its heating rate for industrial oil was 20 °C/min and for RSPE was 33 °C/min (Figure 3). In the same time, the heating rate for Sulfanol was 2 °C/min and for ViscoCrete 2100 was 11 °C/min (Figure 3). Two key differences can explain this difference in the heating rate of the dispersed systems in question using the USD of the aqueous and the organic medium: different absorption coefficients of ultrasonic energy, and coefficients of heat capacity. All other things being equal, the heating rate of the dispersed solution is inversely proportional to its heat capacity:

$$\Delta T = \frac{aM_u t_u}{C_m m}, \quad (14)$$

where  $a$ —the sound energy absorption coefficient;  $M_u$ —the ultrasound source power;  $t_u$ —the duration of the USD;  $C_m$ —the disperse solution heat capacity (medium);  $m$ —the disperse system mass (medium).

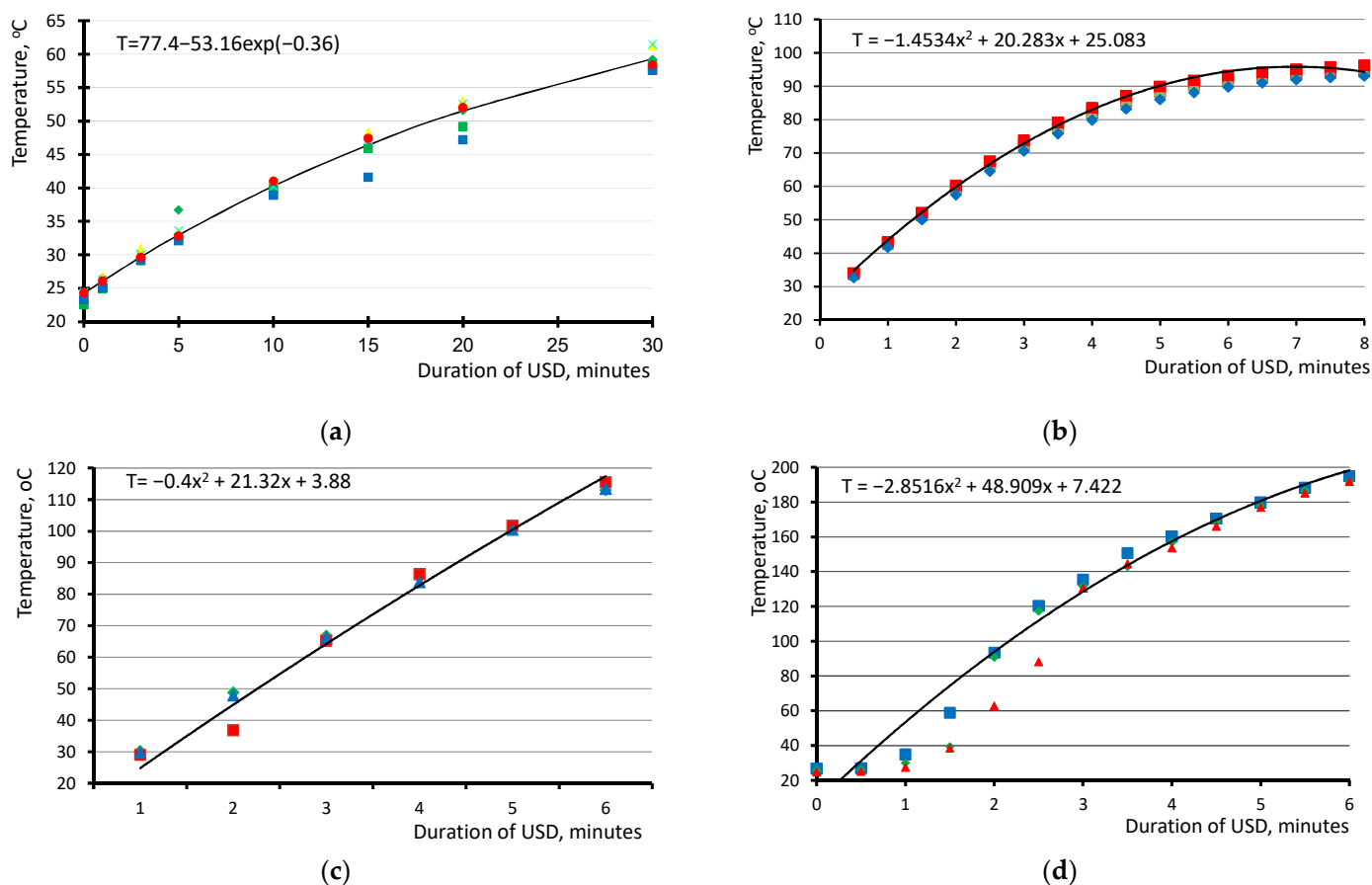


**Figure 6.** Dependence of solution (for each concentration in range) temperatures on the duration of USD: (a) aqueous (MFN and Sulfanol); (b) aqueous (CNPLUS and ViscoCrete 2100); (c) organic (MWCNT and industrial oil); (d) organic (MWCNT-MD and RSPE).

The heat capacity of water is usually always greater than the heat capacity of organic liquids. When the heat capacity of the medium decreases, the heating rate will be higher. The equation presented also implies a direct proportional dependence on the duration of ultrasound. However, this is not observed for the studied dispersed systems. The obvious reasons for this are: (1) USD is not performed under adiabatic conditions. Therefore, with an increase in the temperature gradient, the amount of heat transferred to the environment also increases, the more intense the greater this temperature gradient; (2) The absorption coefficient of ultrasonic energy for dispersed systems may not be a constant value but may depend on the parameters of the system structure.

For the aqueous systems “MFN-Sulfanol” and “MWCNT CNPLUS—ViscoCrete 2100”, heating will have a negative effect, since according to the Gibbs equation:

$$\Gamma = -\frac{c}{RT} \left( \frac{\partial \sigma}{\partial c} \right)_T' \quad (15)$$

(where  $c$ —the surfactant concentration;  $T$ —the temperature;  $R$ —the universal gas constant) an increase in temperature will lead to a decrease in the amount of surfactant adsorption and an increase in the intensity of particle collisions, which together will lead to their aggregation. The particle size were determined using a Zetatrac laser analyzer, which allows reliably determining particle size up to 0.8 nm (Figures 7 and 8).

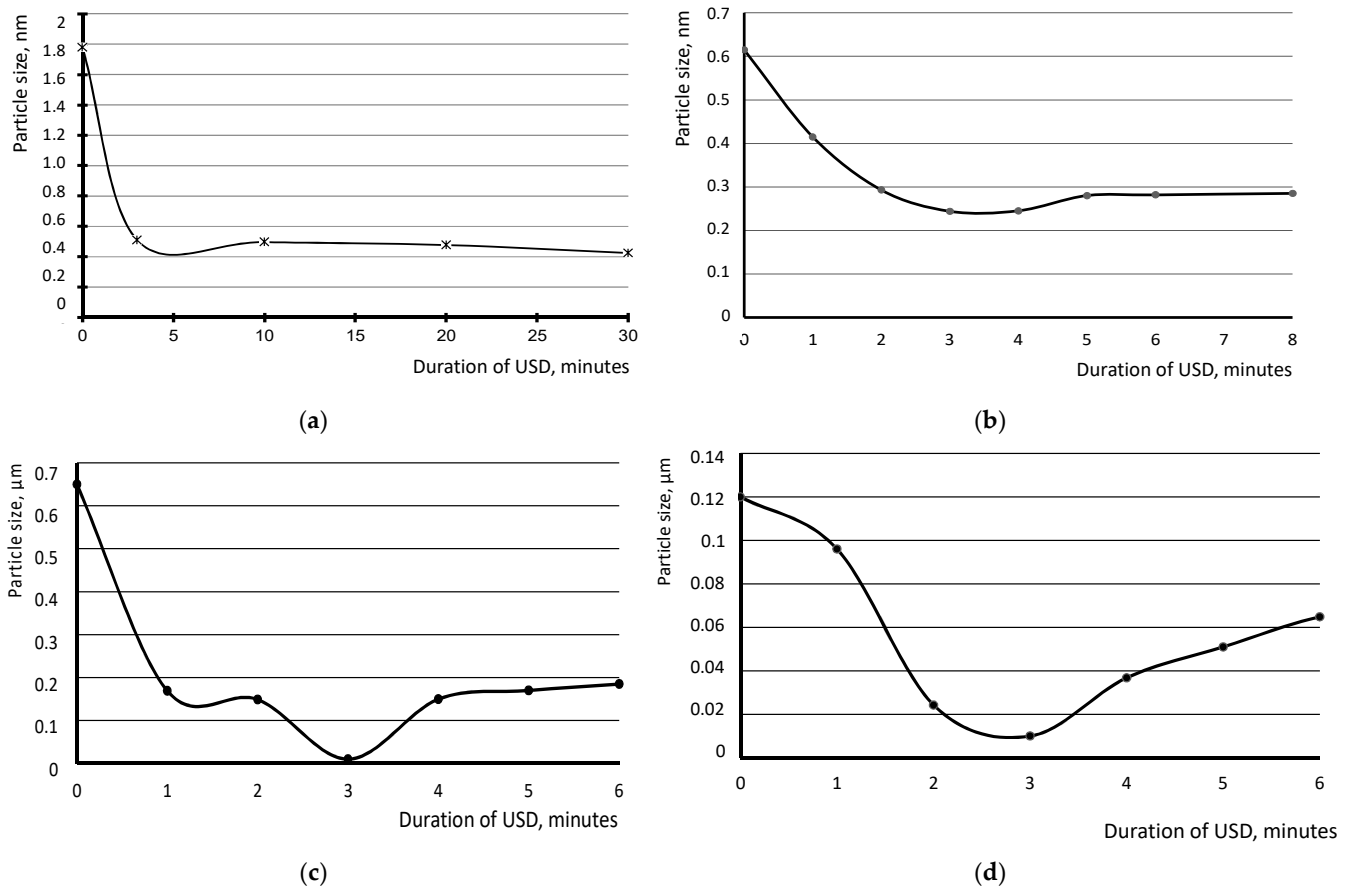


**Figure 7.** Change in the average particle size from the duration of the USD: (a) aqueous (MFN and Sulfanol); (b) aqueous (CNPLUS and ViscoCrete 2100); (c) organic (MWCNT and industrial oil); (d) organic (MWCNT-MD and RSPE).

It is seen from the presented Figure 7a that the most intensive change in MFN particle size of (in the studied range, Table 3) in aqueous solution with Sulfanol is observed in the first 3 min of ultrasonication. At initial unit sizes above 1.8 microns after dispersion reach 0.51 microns. There is also a significant increase in the particle size below 100 nm in this time range (Figure 8a). Further ultrasonic treatment does not result in increase dispersion efficiency. The diameter ranges from 0.4 to 0.6 microns. The total content of MFN particles with dimensions less than 100 nm does not exceed 15%. It is seen from the presented Figure 7b that the most significant changes in the size of CNPLUS particles in an aqueous solution with ViscoCrete 2100 also occur within the first 3 min of USD. Resulting in reduced particle sizes from 0.6 microns to 0.24 microns. At the same time, there is a significant increase in particles smaller than 100 microns (Figure 8b). Further ultrasonic treatment does not result in increase dispersion efficiency. The diameter of the agglomerate ranges from 0.24 to 0.3 microns. The total content of MWCNT CNPLUS particles with dimensions less than 100 microns does not exceed 16%.

It is seen from the presented Figure 7c,d that the maximum USD effect for organic media with MWCNT and MWCNT-MD are also achieved within the first 3 min. Which results in a reduction in size from 0.65 microns to 0.062 microns for industrial oil and to 0.01 microns for RSPE. This confirms the effectiveness of dispersion of MWCNT and MWCNT-MD. Further ultrasonication results in aggregation of particles and is not effective. So, in the third minute of USD, the content of particles smaller than 100 nm reaches 92% (Figure 8c) and 100% (Figure 8d), respectively. Further dispersion reduces the size of particles below 100 nm to 80% and 96%.

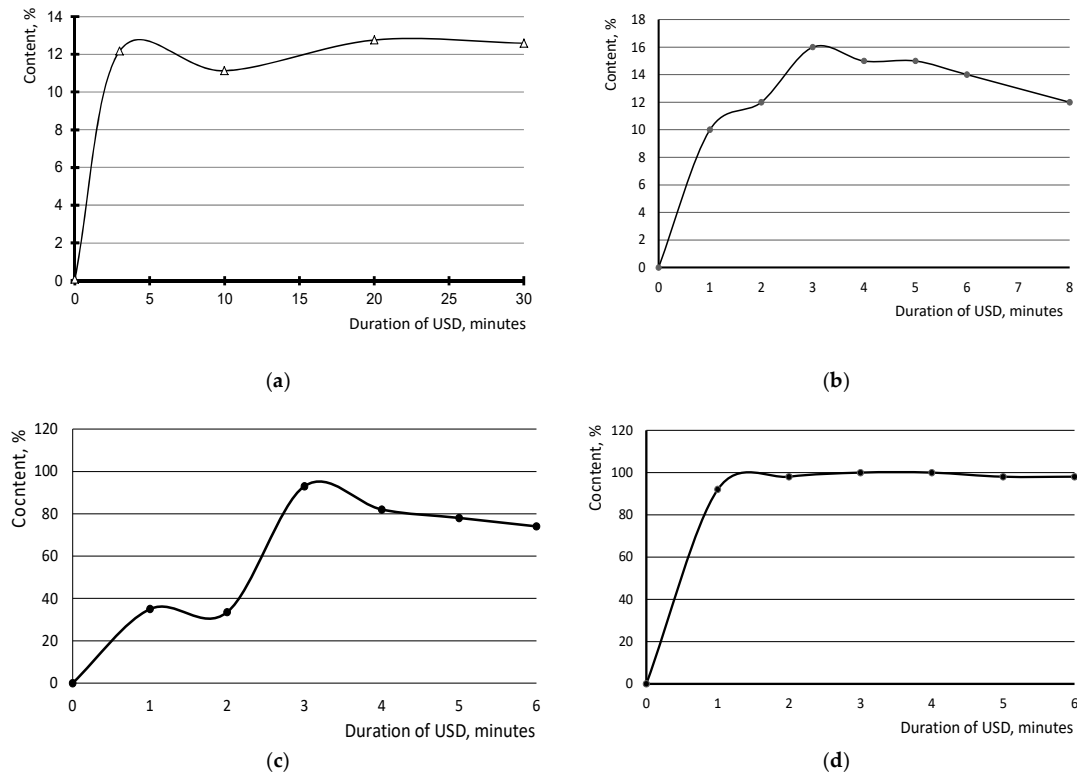


**Figure 8.** Change in the particle content <100 nm from the duration of the USD: (a) aqueous (MFN and Sulfanol); (b) aqueous (CNPLUS and ViscoCrete 2100); (c) organic (MWCNT and industrial oil); (d) organic (MWCNT-MD and RSPE).

The uneven distribution of particles in the aqueous medium can be coiled by the energy dependence of the interaction between particles on their distance (Figure 9). When the powder is mixed with the liquid (even if the powder is hydrophilic) wetting of its surface leads as a rule to “sliding” the particles at a distance  $R$ . Further mixing allows increase the distance to  $R_2$ . However, average distance in disperse systems tend to be larger than  $R_2$ . Therefore, cluster groups with a distance between  $R_2$  particle surface are formed. They require additional mixing energy to break, which causes the number of particles in the cluster to change. Clusters can be destroyed in prolonged mixing. This explains the laboriousness of creating a dispersed system with a uniform (or close to it) particle distribution by mass.

The efficiency of ultrasonic dispersion depends on the intensity of ultrasonic vibrations and the conditions of their propagation. The determination of the allowable intensity range at which ultrasonic dispersion is required depending on the initial viscosity, the consistency index  $K$  and the nonlinearity of the liquid phase  $N$  can be determined from the equation of dynamics of a single bubble for the expansion stage (Equation (16)) and the Kirkwood–Bethe equation for the collapse stage [33]:

$$\frac{3}{2} \left( \frac{\partial R}{\partial t} \right)^2 R \frac{\partial^2 R}{\partial t^2} = - \frac{4\mu_0}{\rho_0} \left[ 1 + \left( \frac{K}{2\mu_0} \right) \left( \frac{6 \left( \frac{\partial R}{\partial t} \right)^2}{R^2} \right)^{\frac{|N|}{2}} \right]^{-\text{sgn}N} \frac{\partial R}{R} + \left( \frac{p_0}{\rho_0} + \frac{2\sigma}{\rho_0 R_0} \right) \left( \frac{R_0}{R} \right)^{3\gamma} + \frac{p_{\Pi} - p_0 + \sqrt{2\rho_0 c} \sin(2\pi f t) + F}{\rho_0}, \tag{16}$$

where  $R$ —the instant radius of the cavitation bubble, m;  $\rho_0$ —the density of the liquid phase, kg/m<sup>3</sup>;  $R_0$ —the radius of the cavitation embryo, m;  $\gamma$ —the adiabatic index in a gaseous medium;  $\sigma$ —the surface tension of the liquid phase, N/m;  $\rho$ —the density of the cavitating heterogeneous medium, kg/m<sup>3</sup>;  $c$ —the speed of sound in a cavitating medium,

$m/c$ ;  $I$ —the intensity of ultrasonic vibrations in the vicinity of the cavitation bubble,  $W/m^2$ ;  $p_0$ —the static pressure in the treated medium, Pa;  $f$ —the frequency of ultrasonic vibrations, Hz;  $F$ —the a function characterizing the nonlinear viscous properties of the liquid phase surrounding the cavitation bubble,  $kg/(m \cdot c^2)$  (for linearly viscous liquids it is equal to 0).

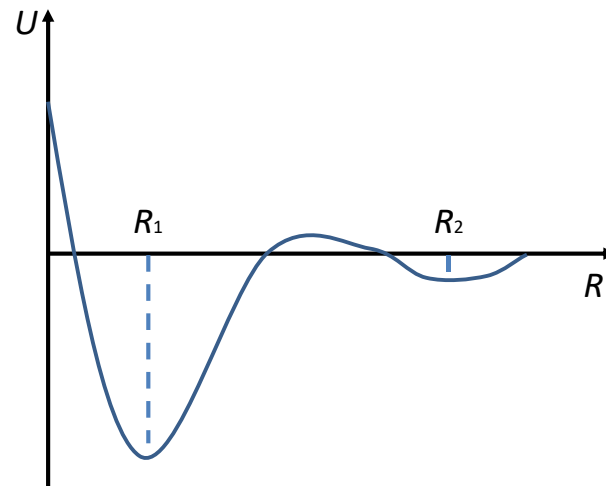


**Figure 9.** The energy dependence of the interaction between particles on their distance.  $U$ —energy of interaction between particles;  $R_1$ —distance of the nearest potential holes (near coagulation);  $R_2$ —distance of the farther potential holes (distant coagulation).

In this range, bubbles break. Shock waves formed without bubbles degenerate into long-lived radial oscillations near the medium radius. Long-lived bubbles formation will occur at an intensity exceeding the maximum detected allowable range. However, at the boundary intensities of the range, the force of shock waves generated by a set of cavitation bubbles tends to reach zero [34]. This will reduce the efficiency of the ultrasound treatment. It has been determined that there is a narrower range of optimal capacities.

An important characteristic of the cavitation efficiency measure is the absorption coefficient (Equation (17)). Its value is proportional to the total power of the shock waves of cavitation bubbles. It is defined by the formula [35]:

$$K_* = -\frac{\omega}{c_0} \operatorname{Im} \frac{\rho_0 c_0^2 \bar{\delta}_1}{(\sqrt{2\rho c I}) e^{i\varphi}}; I = \frac{|\bar{p}_1|^2}{2\rho c}; \bar{p}_1 = |\bar{p}_1| e^{i\varphi}; \bar{\delta}_1 = \frac{\omega}{2\pi} \int_0^{\frac{2\pi}{\omega}} \delta(t) e^{-i\omega t} dt, \quad (17)$$

where  $\varphi$ —the phase shift of sound pressure  $\bar{p}_1$ , rad;  $t$ —the time,  $c$ ;  $\rho_0$ —the density of the liquid phase,  $kg/m^3$ ;  $c$ —the speed of sound in a cavitating medium,  $m/c$ ;  $\omega$ —the circular frequency of ultrasonic vibrations,  $c^{-1}$ ;  $\delta(t)$ —the instant value of the volume content of bubbles in a liquid;  $\rho$ —the density of the cavitating medium,  $kg/m^3$ ;  $c_0$ —the speed of sound in the liquid phase,  $m/c$ .

So, in [35,36] it was found that the dependence of the absorption coefficient on the intensity of the impact is characterized by an extremum, the value of which determines the optimal intensity of the ultrasonic effect, since during this period the maximum transformation of the energy of the primary ultrasonic wave into the energy of shock waves created by cavitation bubbles occurs. Using these results for the analysis of cavitation zones in the chambers of the ultrasonic dispersant, it is possible to establish optimal exposure conditions. An additional tool for improving the efficiency of ultrasonic dispersion is to control the shape of the surface of the bath of the apparatus in which the treatment is performed.

In aqueous systems, when exposed to ultrasound, it was not possible to disperse the dispersed phase to a size of less than 100 nm. To establish the influence or no influence of this fact on the final properties of the composite, samples of concrete mortar were prepared. For each CNPLUS content (0%, 0.005%, 0.01% by weight of cement), 9 samples were made,

and 3 samples were tested at each age of hardening (7, 14 and 28 days). The strength indicators of concrete samples obtained on days 7, 14, and 28 are presented in Figure 10.

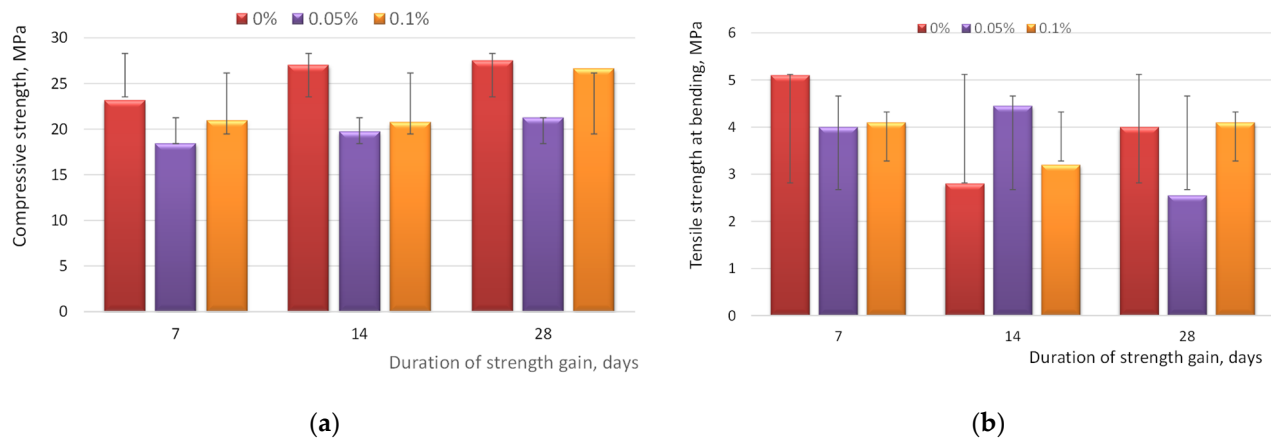


**Figure 10.** The effect of CNPLUS content on the strength parameters of concrete mortar: (a) compressive strength; (b) tensile strength during bending.

It is seen from the presented Figure 10 that the introduction of CNPLUS has no effect on the compressive strength. The uneven distribution of CNPLUS in an aqueous medium with ViscoCrete 2100 (visible particle deposition) was reflected in the static data spread on compressive and bending strength. The effect of MWCNT-MD on the properties of polymer-modified binders (Table 6) was evaluated on the following compositions, Table 7.

**Table 6.** Physical and mechanical characteristics of polymer-modified binder (PMB).

Name of Characteristic	RUSSIAN STATE STANDART 52056-2003, PMB 60	Studied Compositions of PMB				
		No. 1	No. 2	No. 3	No. 4	No. 5
Needle penetration depth, mm <sup>-1</sup> , T 25 °C	no less 60	75	75	77	80	82
Needle penetration depth, mm <sup>-1</sup> , T 0 °C	no less 32	34	35	32	34	31
Ductility, cm, T 0 °C	no less 11	15	18	13	16	13
Ring and ball softening temperature, °C	no less 54	66	67	63	66	61
Fraas fragility temperature, °C	no more -20	-27	-28	-23	-27	-22
Change in softening temperature after thermo-oxidative aging, °C	no more 5	4.57	1.04	1.80	1.5	1.95
Change in fragility temperature after thermo-oxidative aging, °C	–	3.00	1.81	2.11	1.97	2.51
Homogeneity	homogeneous			homogeneous		

**Table 7.** Component composition of polymer-modified binder (PMB).

Composition Number	Name of Component and Content, %			
	Bitumen 100/130	SBS-L	Residual Selective Purification Extract	MWCNT-MD
1	100	4.5	2.0	–
2	100	3.5	2.0	0.005
3	100	3.5	2.0	0.0005
4	100	3.0	2.0	0.005
5	100	3.0	2.0	0.0005

Composition No. 1 was developed with a different plasticizer by the authors of the study earlier [20], where it was also found that the introduction of a nano-modifier reduces the polymer content in the polymer-modified binder, therefore, compositions 2 and 3 were prepared with a lower polymer content by 23% and compositions 4 and 5 were prepared with a lower polymer content by 33%.

The shear rate (90 s<sup>-1</sup>) is selected from a range that does not contribute to the value of the dynamic viscosity of the studied PBB samples. It is seen from the presented Table 5 that the use of RSPE as a medium of MWCNT-MD, allows for an improvement in the physical and mechanical characteristics of the polymer-modified binders with a reduced polymer content by 33% (composition No. 4), as well as to ensure the stability of the structure

and improve resistance to destructive processes. So, the intensity of changes in high-temperature characteristics after the thermo-oxidative aging process decreased by more than 4 times, the intensity of changes in low-temperature characteristics after the thermo-oxidative aging process decreased by more than 1.5 times. The analysis of rheological characteristics (Table 8) shows that the organic medium with MWCNT-MD nanoparticles evenly distributed in it, provides the structuring of the PMB system (composition No. 4), such as composition No. 1, with a high polymer content (by 33%).

**Table 8.** Dynamic viscosity [Pa·s] of polymer-modified binder at a shear rate of  $90 \text{ s}^{-1}$ .

Temperature, °C	Studied Compositions of PMB				
	No. 1	No. 2	No. 3	No. 4	No. 5
100	8.08	8.20	7.51	8.07	7.40
135	1.03	1.29	0.84	1.02	0.76
160	0.30	0.32	0.28	0.30	0.25

#### 4. Conclusions

In the present study, physical processes occurring in dispersed media with carbon nanomaterials under the influence of an ultrasonication were investigated. Moreover, residual selective purification extract was successfully used to obtain a high-quality dispersion of CNTs organic suspension. Using this route, we studied the influence of the surfactant with added CNTs concentration, sonication time, temperature and surface adsorption activity.

The results of laser spectroscopy, CNTs bundle size measurement and surface tension of surfactants' molecules, showed that using the anionic surfactants (Sulfanol, ViscoCrete 2100) resulted in surfactant molecules are adsorbed on the surface of CNTs in the aqueous dispersive medium. However, it was not enough to result in a highly homogeneous and full stabilization of CNTs in the aqueous dispersive medium.

The results of laser spectroscopy, CNTs bundle size measurement and surface tension of surfactants' molecules, showed that using the organic hydrocarbon medium (industrial oil, residual selective purification extract) resulted in a highly homogeneous and full stabilization of CNTs in the organic dispersive medium, at the expense of being under the molecular separation of the polymolecular medium because of interaction with MWCNT-MD.

It was established that ultrasonic treatment has a more intensive effect in an organic hydrocarbon medium, (industrial oil, residual selective purification extract). So, in industrial oil, the heating rate from USD is  $20 \text{ °C/min}$ , in RSPS it is  $33 \text{ °C/min}$ . For aqueous systems, the heating rate from USD is significantly lower and amounts to  $2 \text{ °C/min}$  for suspensions with Sulfanol and  $11 \text{ °C/min}$  for suspensions with ViscoCrete 2100. The obvious reasons for this are: (1) USD is not performed under adiabatic conditions, therefore, with an increase in the temperature gradient, the amount of heat transferred to the environment also increases, the more intense, the greater this temperature gradient; (2) The absorption coefficient of ultrasonic energy for dispersed systems may not be a constant value but may depend on the parameters of the system structure.

Based on the results of the determination of the average sizes of carbon materials in various media by means of laser diffractometry, it was established that the greatest effect from ultrasonic action is observed during the first three minutes. In the aqueous solution, the median diameter of MFN of  $0.51 \text{ }\mu\text{m}$  and the median diameter of CNPLUS of  $0.24 \text{ }\mu\text{m}$  was achieved. The decrease in the effectiveness of the USD with increasing its duration is explained by the reduction in the adsorption activity of Sulfanol and ViscoCrete 2100 with increasing temperature. In the organic media, it was possible to achieve the nanoscale dispersion of MWCNT agglomerates the average size of  $62 \text{ nm}$  (for industrial oil) and  $9 \text{ nm}$  (for residual selective purification extract). It was established that the greatest effect from ultrasonic action is shown in a medium characterized by lower surface tension forces, lower density, and higher intensity of heating from the USD.

It was established that use of the residual selective purification extract with MWCNT-MD, allows for an improvement in the physical and mechanical characteristics of the polymer-modified binder with a reduced polymer content by 33%, as well as to ensure the stability of the structure and improve resistance to destructive processes.

**Author Contributions:** Conceptualization, S.O. and E.K.; methodology, validation, formal analysis, investigation, data curation, writing—original draft preparation, S.O.; writing—review and editing, supervision, E.K. All authors have read and agreed to the published version of the manuscript.

**Funding:** Financial support for this work was obtained from Russian Science Foundation contract numbers: 21-79-00191, <https://rscf.ru/en/project/21-79-00191/>.

**Institutional Review Board Statement:** Not applicable.

**Informed Consent Statement:** Not applicable.

**Data Availability Statement:** Data are contained within the article.

**Conflicts of Interest:** The authors declare no conflict of interest.

## References

- Konsta-Gdoutos, M.S.; Metaxa, Z.S.; Shah, S.P. Multi-scale mechanical and fracture characteristics and early-age strain capacity of high-performance carbon nanotube/cement nanocomposites. *Cem. Concr. Compos.* **2010**, *32*, 110–115. [[CrossRef](#)]
- Tugelbayev, A.; Kim, J.-H.; Lee, J.U.; Chung, C.-W. The effect of acid treated multi-walled carbon nanotubes on the properties of cement paste prepared by ultrasonication with polycarboxylate ester. *J. Build. Eng.* **2023**, *64*, 105638. [[CrossRef](#)]
- Kim, G.M.; Nam, I.W.; Yang, B.; Yoon, H.N.; Lee, H.K.; Park, S. Carbon nanotube (CNT) incorporated cementitious composites for functional construction materials: The state of the art. *Compos. Struct.* **2019**, *227*, 111244. [[CrossRef](#)]
- Shekhovtsova, S.; Korolev, E.V. Formation of polymer modified binder structure in the presence of carbon nanomaterials. *Constr. Build. Mater.* **2021**, *303*, 124591. [[CrossRef](#)]
- Zhang, F.; Cao, Y.; Sha, A.; Wang, W.; Song, R.; Lou, B. Mechanism, rheology and self-healing properties of carbon nanotube modified asphalt. *Constr. Build. Mater.* **2022**, *346*, 128431. [[CrossRef](#)]
- Yang, Q.; Li, X.; Zhang, L.; Qian, Y.; Qi, Y.; Kouhestani, H.S.; Shi, X.; Gui, X.; Wang, D.; Zhong, J. Performance evaluation of bitumen with a homogeneous dispersion of carbon nanotubes. *Carbon* **2020**, *158*, 465–471. [[CrossRef](#)]
- Stynoski, P.; Mondal, P.; Marsh, C. Effects of silica additives on fracture properties of carbon nanotube and carbon fiber reinforced Portland cement mortar. *Cement Concr. Compos.* **2015**, *55*, 232–240. [[CrossRef](#)]
- Xu, S.; Liu, J.; Li, Q. Mechanical properties and microstructure of multi-walled carbon nanotube-reinforced cement paste. *Construct. Build. Mater.* **2015**, *76*, 16–23. [[CrossRef](#)]
- Andrievsky, R.A. Nanostructured materials—The state of development and prospects. *Perspect. Mater.* **2001**, *6*, 5–11.
- Korolev, E.V.; Kuvshinova, M.I. Ultrasound parameters for homogenization of dispersed systems with nanoscale modifiers. *Stroit. Mater.* **2010**, *9*, 85–88.
- Elpiner, I.E. *Biophysics of Ultrasound*; Science: St. Petersburg, Russia, 1973; pp. 134–384.
- Brennen, C.E. *Cavitation and Bubble Dynamics*; Oxford University Press: Cary, NC, USA, 1995; 84p.
- Kikuchi, E. *Ultrasound Transducers*; Mir: Moscow, Russia, 1972; 424p.
- Margulis, M.A. *Sound Chemical Reactions and Sonoluminescence*; Chemistry: Moscow, Russia, 1986; 300p.
- Golyamina, I.P. *Ultrasound. A Small Encyclopedia*; High School: Moscow, Russia, 1986; 280p.
- Khmelev, V.N.; Golikh, R.N.; Shalunov, A.V.; Khmelev, S.S. Increase of efficiency of ultrasonic influence on heterogeneous systems with a carrier liquid phase of high viscosity. *South-Sib. Sci. Bull.* **2013**, *2*, 10–15.
- Verezhnikov, V.N. *Selected Chapters of Colloid Chemistry*; Rostov State University: Rostov-on-Don, Russia, 2011; 237p.
- Bag, N.; Kammakam, I.; Falath, W. Nanomaterials: A review of synthesis methods, properties, recent progress, and challenges. *Mater. Adv.* **2021**, *2*, 1821–1871. [[CrossRef](#)]
- Kazemzadeh, Y.; Shojaei, S.; Riazi, M.; Sharifi, M. Review on application of nanoparticles for EOR purposes: A critical review of the opportunities and challenges. *Chin. J. Chem. Eng.* **2019**, *27*, 237–246. [[CrossRef](#)]
- Shekhovtsova, S.; Korolev, E.V. Nanomodified rejuvenators and protective materials for asphalt concrete. *Mag. Civ. Eng.* **2021**, *106*, 10607.
- Rennhofer, H.; Zanghellini, B. Dispersion State and Damage of Carbon Nanotubes and Carbon Nanofibers by Ultrasonic Dispersion: A Review. *Nanomaterials* **2021**, *11*, 1469. [[CrossRef](#)]
- Liu, J.; Zhao, L.; Chi, L.; Luo, G.; Li, T.; Cai, S. Effect of multilayer graphene oxide on the hydration and early mechanical strength of cement mortar in low temperature. *Constr. Build. Mater.* **2023**, *364*, 129997. [[CrossRef](#)]
- Guo, S.-Y.; Luo, H.-H.; Tan, Z.; Chen, J.-Z.; Zhang, L.; Ren, J. Impermeability and interfacial bonding strength of TiO<sub>2</sub>-graphene modified epoxy resin coated OPC concrete. *Prog. Org. Coat.* **2021**, *151*, 106029. [[CrossRef](#)]

24. Sesis, A.; Hodnett, M.; Memoli, G.; Wain, A.J.; Jurewicz, I.; Dalton, A.B.; Carey, J.D.; Hinds, G. Influence of Acoustic Cavitation on the Controlled Ultrasonic Dispersion of Carbon Nanotubes. *J. Phys. Chem. B*. **2013**, *117*, 15141–15150. [[CrossRef](#)]
25. Yadav, P.; Gupta, S.M.; Sharma, S.K. A review on stabilization of carbon nanotube nanofluid. *J. Therm. Anal. Calorim.* **2022**, *147*, 6537–6561. [[CrossRef](#)]
26. Manzetti, S.; Gabriel, C.P. Methods for dispersing carbon nanotubes for nanotechnology applications: Liquid nanocrystals, suspensions, polyelectrolytes, colloids and organization control. *Int. Nano Lett.* **2019**, *9*, 31–49. [[CrossRef](#)]
27. Eatemadi, A.; Daraee, H.; Karimkhanloo, H.; Kouhi, M.; Zarghami, N.; Akbarzadeh, A.; Abasi, M.; Hanifehpour, Y.; Joo, S.W. Carbon nanotubes: Properties, synthesis, purification, and medical applications. *Nanoscale Res. Lett.* **2014**, *9*, 393. [[CrossRef](#)] [[PubMed](#)]
28. Yang, K.; Wu, W.; Jing, Q.; Jiang, W.; Xing, B. Competitive adsorption of naphthalene with 2, 4-dichlorophenol and 4-chloroaniline on multiwalled carbon nanotubes. *Environ. Sci. Technol.* **2010**, *44*, 3021–3027. [[CrossRef](#)] [[PubMed](#)]
29. Rather, S.U. Preparation, characterization and hydrogen storage studies of carbon nanotubes and their composites: A review. *Int. J. Hydrog. Energy* **2020**, *45*, 4653–4672. [[CrossRef](#)]
30. Ponomarev, A.N.; Nikitin, V.A.; Rybalko, V.V. Investigation of multilayer polyhedral nanoparticles of fulleroid type—Astralenes. *J. Surf. Investig. X-ray Synchrotron Neutron Tech.* **2006**, *5*, 44–47.
31. Kuznetsov, V.A.; Papinova, A.V.; Kushchev, P.O.; Shatalov, G.V. Self-organizing systems of poly-n-vinylpyrrolidone-sulfanol in dilute aqueous solutions. *Bull. Voronezh State Univ. Ser. Chem. Biol. Pharm.* **2015**, *3*, 10–15.
32. Shekhovtsova, S.; Vysotskaya, M.; Korolev, E.; Inozemtcev, S. Development of aggregationally and sedimentationally resistant nanosuspension for efficient polymer modified bitumen. *IOP Conf. Ser. Mater. Sci. Eng.* **2018**, *365*, 032008. [[CrossRef](#)]
33. Time, R.W.; Rabenjafimanantsoa, A.N. Cavitation Bubble Regimes in Polymers and Viscous Fluids. *Annu. Trans. Nord. Rheol. Soc.* **2011**, *19*, 12.
34. Khmelev, V.N.; Golykh, R.N.; Shalunov, A.V. Optimization of these modes and conditions of ultrasonic influence on various technological mediums by mathematical modeling. In Proceedings of the International Conference and Seminar of Young Specialists on Micro/Nanotechnologies and Electron Devices, Altai, Russia, 2–6 July 2012; pp. 124–128.
35. Margulis, M.A.; Margulis, I.M. Dynamics of ensemble of bubbles in the cavitating fluid. *J. Phys. Chem.* **2007**, *81*, 2290–2295.
36. Golikh, R.N.; Khmelev, V.N.; Khmelev, S.S.; Barsukov, R.V.; Shalunov, A.V. Simulation of the process of formation of the cavitation region in viscous liquids to determine the optimum process volume to be processed and the impact regimes. *News High. Educ. Inst. Chernozem Reg.* **2010**, *4*, 58–62.

**Disclaimer/Publisher’s Note:** The statements, opinions and data contained in all publications are solely those of the individual author(s) and contributor(s) and not of MDPI and/or the editor(s). MDPI and/or the editor(s) disclaim responsibility for any injury to people or property resulting from any ideas, methods, instructions or products referred to in the content.